INVERSION OF THE LIDAR EQUATION PROVIDING FOR SMALL-ANGLE SCATTERING

D.V. Vlasov, E.V. Zubkov, and S.I. Shamaev

Central Scientific-Production Association "Kometa," Moscow
Russian Committee on Defense Industry
Received June 8, 1994

A modified solution of the lidar equation has been derived that develops the Klett algorithm as a stable form of inversion of the lidar equation and provides the reconstruction of the extinction coefficient profiles from laser sounding data. This solution allows for the small-angle scattering typical of oceanic waters. Inversion errors for the Klett and modified algorithms have been compared in a numerical lidar experiment for a medium with various model vertical profiles of the extinction coefficient.

In general, inverse problem of laser sounding of oceanic medium, which involves the reconstruction of the vertical profiles of hydro-optical characteristics from backscatter signals, is an ill-posed problem from the mathematical standpoint.

This is caused by effects of multiple scattering of a collimated laser beam in an inhomogeneous (both by the volume concentration and size distribution of scatters) medium, which are difficult to consider, as well as by double passage of radiation trough a random oceanic surface.[1]

Laser aerosounding of oceanic medium is used to solve a number of applied problems. In this case, as a rule, relative measurements of the hydro-optical characteristics are of interest, especially their spatial distribution and spatiotemporal variability of different scales; at the same time, measurement of the absolute values is not important.

Proceeding from objectives of applied studies, approaches to the inverse problem solution are based on the use of approximate expressions allowing to one or another extent for the specific character of laser sounding of the upper oceanic layer and, at the same time, being sufficiently simple to satisfy the requirements for real-time processing.

One of these approaches is the Klett algorithm[2–4] allowing the inversion of the lidar equation for the extinction coefficient to be realized. This algorithm was used to process backscatter signals of both the atmosphere[2] and oceanic[5] media.

The papers devoted to analysis of possibilities and peculiarities of the given algorithm are known.[6–9]

In Ref. 2, the lidar equation

$$P(r) = P_{\rm p} \frac{c\,\tau_{\rm p}}{2} \Phi \frac{\sigma(\pi, r)}{r^2} \exp\left[-2 \int_0^r \varepsilon(l)\, {\rm d}l \right] \qquad (1)$$

was used, where $P_{\rm p}$ is the pulse power, $\tau_{\rm p}$ is the pulse duration, c is the velocity of light, Φ is the effective area of a receiving antenna, σ is the scattering coefficient, r is the distance along a sounding path, $\sigma(\pi, r)$ is the backscattering coefficient, $\varepsilon(r) = \sigma(r) + \varkappa(r)$ is the extinction coefficient, and $\varkappa(r)$ is the absorption coefficient. Equation (1) is solved for $\varepsilon(r)$ on the assumption that

$$\sigma = B\, \varepsilon^k , \qquad (2)$$

where B and k are the constants with the value of k being within the interval 0.67–1.0 depending on the type of scattering particles.

Klett[2] obtained the stable solution

$$\varepsilon(r) = \frac{\exp\left(\dfrac{S(r) - S_m}{k}\right)}{\dfrac{1}{\varepsilon_m} + \dfrac{2}{k} \displaystyle\int_r^{r_m} \exp\left(\dfrac{S(r') - S_m}{k}\right) {\rm d}r'} , \qquad (3)$$

where $S(r) = \ln[P(r)\, r^2]$ is the logarithm of the backscatter signal power $P(r)$ weighted with distance, r_m is the maximum distance along the sounding path, $\varepsilon_m = \varepsilon(r_m)$, and $S_m = S(r_m)$. However, as noted by Klett himself,[2] solution (3) ignores the small-angle scattering effects and, we add, the effects of double passage of radiation through a random interface between media. Since rigorous (with allowance for these effects) expression for echo-signal power[1] cannot be analyzed numerically in practice, the necessity arises to search for approximate solutions.

To take into account the small-angle scattering in the solution (3), we use the expression known from the papers of Dolin and Savel'ev (Ref. 10)

$$s(r) = s_0(r) + \pi \int_0^r \gamma_0^2(\xi)\, \sigma(\xi)\, (r - \xi)^2\, {\rm d}\xi , \qquad (4)$$

which describes variations of the beam cross section (in the small-angle approximation) in an inhomogeneous

0235-6880/95/09 706-05 $02.00

scattering medium. In Eq. (4) $s_0(r) = \pi(r \tan\alpha_\Lambda)^2$ is the beam cross section ignoring the scattering, α_Λ is the angular beam divergence, and $\gamma_0^2(\xi)$ is the variance of the angle of deflection due to a single act of scattering.

In this case, the following assumptions were made.

1. Sounding is carried out from the height H through a smooth interface between media (n_1, σ_1, $\varkappa_1$; n_2, σ_2, $\varkappa_2$); with $n_1 = 1$, $n_2 = n$ (n is the refractive index), $\sigma_1 \ll \sigma_2 = \sigma$, and $\varkappa_1 \ll \varkappa_2 = \varkappa$.

2. The distribution of scatters over size is invariable with depth. This allows one to consider the variance of the angle of deflection due to a single act of scattering to be independent of r:

$$\gamma_0^2(r) = \gamma_0^2 = \text{const} .$$

3. Relation (2) derived by Barteneva[11] and used by Klett is appropriate for a turbid atmosphere (fog, smog, rain cloud) when scattering processes are predominated, and the absorption is small compared with the scattering.

Let us assume that relation (2) is also appropriate for some water types.

Let $\varkappa \le 0.1\,\sigma$, and the mean value $\overline{\varkappa}(\lambda = 530\ \text{nm}) = 0.03\ \text{m}^{-1}$ in accordance with Ref. 12 (p. 185); then $\sigma \ge 0.3\ \text{m}^{-1}$. It seems likely that similar cases (according to classification of water types proposed in Ref. 12) can be observed in regions of drift of eolian suspension, coastal zones, and regions of high bioproductivity of an ocean. This assumption does not contradict the physical model of radiation attenuation (Ref. 12, p. 231) if the relation between $\varkappa$ and σ is estimated based on the photon survival probability

$$\Lambda = \sigma/(\sigma + \varkappa),$$

which is greater or equal to 0.9 for the wavelength range 510–550 nm (for coastal waters) and is 0.77–0.88 (for oceanic waters) to depths as great as 100 m.

If small-scale variability is considered in cross section through the oceanic medium, local formations of such a type can be obviously observed as a fine structure of seasonal thermocline in the form of sublayers of increased turbidity in which the extinction coefficient can change several times.[13]

In connection with the accepted assumption on applicability of relation (2) for some water types, Ref. 5 should be mentioned where results were presented of processing of laser return signals from oceanic medium by various algorithm including the Klett one.

The spread of points on diagrams in the coordinate system (ε, B), where B (in designations from Ref. 5) is proportional to backscattering, shows a presence of various types of functional relations close to linear, between the above quantities.

Within the bounded region of investigations, different water types were observed which are characteristic of areas of river drifts, shallows, and clear waters of oceanic streams. This is manifested through the change of slope of sets of points grouping about some preferred directions in the coordinate system (ε, B) as well as through the shift of these sets of points in the coordinate plane.

4. It is reasonable to assume that the profiles $\sigma(r)$ and $\sigma(\pi, r)$ are correlated since it is well known that basic variations of scattering are primarily caused by changes in the concentration of scattering particles and to a lesser extent by transformation of the particle size distribution.

In their turn, anomalous changes in the concentration of any individual fraction of polydispersed suspension can lead to extrema in the scattering phase function and, as a result, to disagreement between the forms of $\sigma(r)$ and $\sigma(\pi, r)$ profiles. However, as was noted in Ref. 12 (see p. 170), "for most oceanic scattering phase functions, local extrema have not been found.B

Allowing for accepted assumptions for the case of double passage of a collimated beam through the air-water interface, lidar equation (1) can be written in the following form:

$$P(r) = \frac{A\,\sigma(\pi, r) \exp\left[-2\int_0^r \varepsilon(l)\,\mathrm{d}l\right]}{\left[1 + \left(\frac{\nu}{n\,H + r}\right)^2 \int_0^r \sigma(\xi)(r - \xi)^2\,\mathrm{d}\xi\right](n\,H + r)^2}, \tag{5}$$

where $\nu = \gamma_0\, n/\tan\alpha_\Lambda$, and A is the instrumental constant of a lidar.

Using expression (5) and following the procedure of the lidar equation solution described in Ref. 2 in detail, we have derived a modified expression

$$\varepsilon(r) = \frac{\left[\frac{F(r)}{F(r_m)}\right]^{1/k} \exp\left[\frac{S(r) - S_m}{k}\right]}{\frac{1}{\varepsilon_m} + \frac{2}{k}\int_r^{r_m}\left[\frac{F(r)}{F(r_m)}\right]^{1/k} \exp\left[\frac{S(r') - S_m}{k}\right]\mathrm{d}r'}, \tag{6}$$

in which (allowing for the accepted assumptions) the scattering effects are considerated, and

$$F(r) = 1 + \left(\frac{\nu}{n\,H + r}\right)^2 \int_0^r \sigma(\xi)\,(r - \xi)^2\,\mathrm{d}\xi . \tag{7}$$

It should be noted that solution (6) is analogous to the Klett solution[3] if the relation

$$\sigma(r) = B(r)\,[\varepsilon(r)]^k \tag{8}$$

is valid. The difference is that new solution contains the ratio of functionals

$$\left[\frac{F(r)}{F(r_m)}\right]^{1/k}$$

instead of the term $\left[\frac{B(r_m)}{B(r)}\right]^{1/k}$. Numerical modeling of the problem of reconstruction of the $\varepsilon(r)$ profile by modified (6) and known (3) algorithms was carried out for media with different model distribution of $\varepsilon(r)$. The following models were used:

a) homogeneous

$$\sigma(r) = \sigma_0 ; \tag{9}$$

b) linear

$$\sigma(r) = \sigma_0 + a\, r , \tag{10}$$

where $a \gtrless 0$ and $|a| < \sigma_0 / r_m$;

c) exponential

$$\sigma(r) = \sigma_0 \exp(a\, r), \tag{11}$$

in which for $a < 0$ the restriction is imposed

$$|a| = \frac{1}{r_m} \ln\left[\frac{\sigma(r_m)}{\sigma_0}\right]; \tag{12}$$

d) harmonic

$$\sigma(r) = \sigma_0 [1 + m \sin(q\, r)] , \tag{13}$$

where $q = 2\pi / r_0$, and r_0 is the spatial period of variation of $\sigma(r)$;

e) Lorentz model[14]

$$\sigma(r) = \sigma_0 \left\{1 + \frac{\alpha\, \delta^2}{(r - r_0)^2 + \delta^2}\right\} , \tag{14}$$

where r_0 is the coordinate of the maximum concentration of scatters, δ is the half-width of $\sigma(r)$ distribution, and $\alpha \gtrless 0$ is the coefficient determining the maximum value of σ.

Each model has proper functional $F[\sigma(r)]$ found by integration of Eq. (7). Results of integration for $H = 0$ yield:

a) homogeneous model

$$F(r) = 1 + \frac{\sigma_0 \nu^2}{3} r , \tag{15}$$

b) linear model

$$F(r) = \frac{a\, \nu^2}{12} r^2 + \frac{\sigma_0 \nu^2}{3} r + 1 , \tag{16}$$

c) exponential model

$$F(r) = 1 - \left(\frac{\nu}{a\, r}\right)^2 \frac{\sigma_0}{a} [(a\, r + 1)^2 - 2e^{ar} + 1] , \tag{17}$$

d) harmonic model

$$F(r) = 1 + \sigma_0 \left(\frac{\nu}{r}\right)^2 \left\{\frac{r^3}{3} + m \frac{q\, r^2 - 2[1 - \cos(q\, r)]}{q^3}\right\}, \tag{18}$$

e) Lorentz model

$$F(r) = 1 + \sigma_0 \left(\frac{\nu}{r}\right)^2 \left\{\frac{r^3}{3} + \alpha\, \delta^2\, r + \alpha\, \delta[(r - r_0)^2 - \delta^2] \times \right.$$
$$\times \left[\arctan\frac{r - r_0}{\delta} + \arctan\frac{r_0}{\delta}\right] - \alpha\, \delta^2\, (r - r_0) \times$$
$$\left. \times \ln\left[\frac{(r - r_0)^2 + \delta^2}{r_0^2 + \delta^2}\right]\right\} . \tag{19}$$

A simulation program provided the reconstruction of the profile

$$\varepsilon(r) = \sigma(r) + \varkappa \tag{20}$$

in equidistant points of a path whose end points is at r_m by two inversion algorithms: ignoring the scattering effects (3) and allowing for these effects (6).

The following characteristics were calculated beforehand: the true model profile $\varepsilon(r)$ and the simulated value $S(r)$ of the input signal weighted with distance on a logarithmic scale. This value takes into account the effects of multiple small-angle scattering for the given stratification model:

$$S(r) = \ln[P(r)(n\, H + r)^2] = \ln A + \ln[\sigma(\pi, r)] -$$
$$- 2\int_0^r \varepsilon(l)\, dl - \ln\left[1 + \left(\frac{\nu}{n\, H + r}\right)^2 \int_0^r \sigma(\xi)(r - \xi)^2\, d\xi\right] . \tag{21}$$

A program in FORTRAN (for the BESM-6 computer system) provided for double access to algorithm (3) or (6). In the first case, the boundary condition for solution of the lidar differential equation is given by the true value $\varepsilon_m = \varepsilon(r_m)$. In the second case, the problem is approximated to the real situation when the value of ε_m at the end point of the path is *a priori* unknown, and the estimate

$$\hat{\varepsilon}(r_m) = \frac{1}{2} \frac{S_0 - S_m}{r_m - r_0} \tag{22}$$

proposed by Klett[2] is used based on simulated values of real signal.

Reconstruction of the profiles $\varepsilon(r)$ for models (9)–(14) by algorithm (6) with functional $F(r)$ for homogeneous medium (15) simulates most adequately the real situation of remote sensing when *a priori* information on the character of the profile $\varepsilon(r)$ and especially on the value of ε_m at the end point of the path is lacking.

At the same time, preliminary check of algorithm (6) with the use of functionals (15)–(19) for models (9)–(14) have shown a complete coincidence of the initial and reconstructed profiles.

The simulation results are shown in Figs. 1–5. The dashed curve at the top of the figures shows the dependence $S(r)$ (see Eq. (21)).

It follows from the obtained results that ignoring the scattering for the case of homogeneous medium (Fig. 1) results in a relative error of the profile reconstruction (when estimate $\varepsilon = \varepsilon(r_m)$ is used) more than 37% in maximum (curves *1* and *3*), whereas the profile reconstruction by the modified algorithm with $\varepsilon'_m = \hat{\varepsilon}(r_m)$ (curve *4*) provides the error which does not exceed 12% for 84% of the path length.

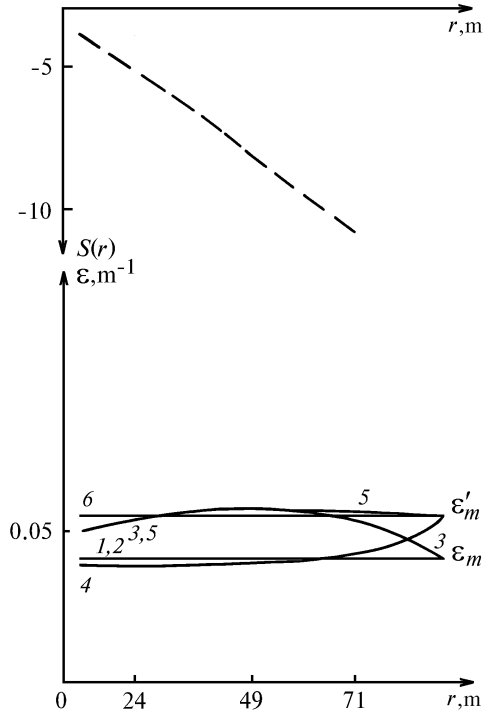

FIG. 1. Comparative results of reconstruction of the $\varepsilon(r)$ *profile for homogeneous model medium (see Eq. (9)) allowing for (modified algorithm) and ignoring (known algorithm) the effects of small-angle scattering with different boundary conditions: true profile of* $\varepsilon(r)$ *(1); reconstruction with boundary conditions given by the true value* $\varepsilon_m = \varepsilon(r_m)$ *(2 and 3); reconstruction with boundary conditions given by the estimate* $\varepsilon'_m = \hat{\varepsilon}(r_m)$ *(from Eq. (22)) (4 and 5); reconstruction allowing for the effects of multiple scattering (modified algorithm (6)) (2 and 4); reconstruction ignoring the effects of multiple scattering (known algorithm (3)) (3 and 5); the level of* ε_m *value for estimate (22) (in Fig. 1 only) (6). S(r) is shown by dashed curves in Figs. 1–5 (see Eq. (21)).*

Figures 2–5 show that the use of the modified algorithm for *a priori* unknown profile (with functional (15) for homogeneous medium) and estimate of the boundary condition $\varepsilon = \varepsilon(r_m)$ ensures small (less than 10-15%) errors in reconstruction (curves *1* and *2* in the figures).

The exception is the region of maximum for the Lorentz model (Fig. 5) where the error increases to approximately 39%. At the same time, this error is still greater, i.e., about 83% (curve *3*) when scattering is ignored.

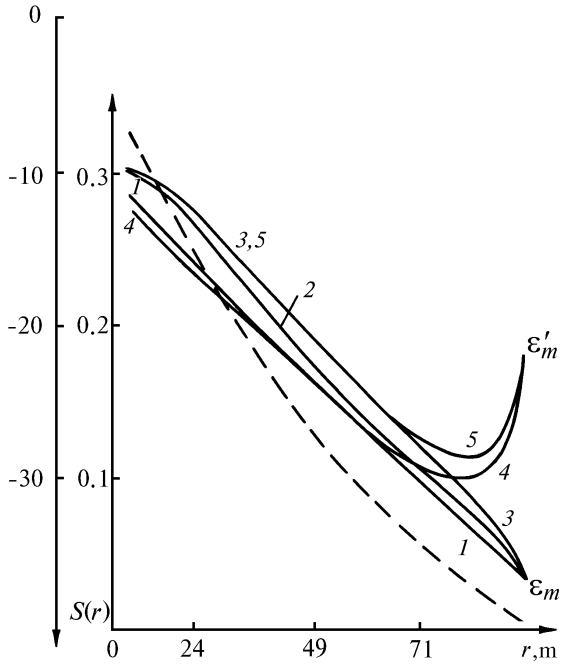

FIG. 2. The same as in Fig. 1 but for the linear model profile $\varepsilon(r)$ *(*$a < 0$*, see Eq. (10)).*

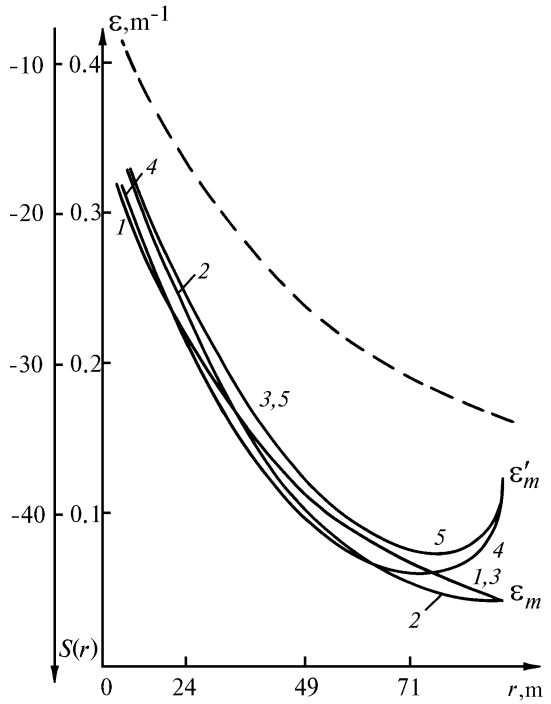

FIG. 3. The same as in Fig. 1 but for the exponential model profile $\varepsilon(r)$ *(*$a < 0$*, see Eqs. (11) and (12)).*

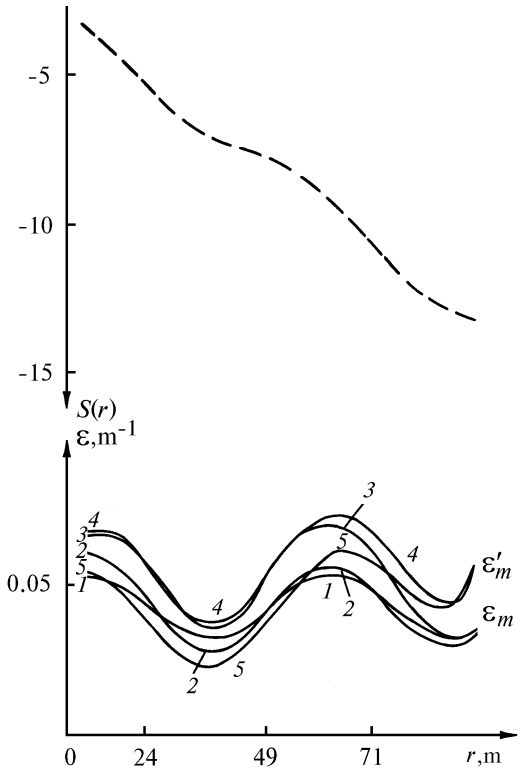

FIG. 4. The same as in Fig. 1 but for the harmonic model profile $\varepsilon(r)$ (r_0 = 50 m, m = 0.5, *see Eq. (13)).*

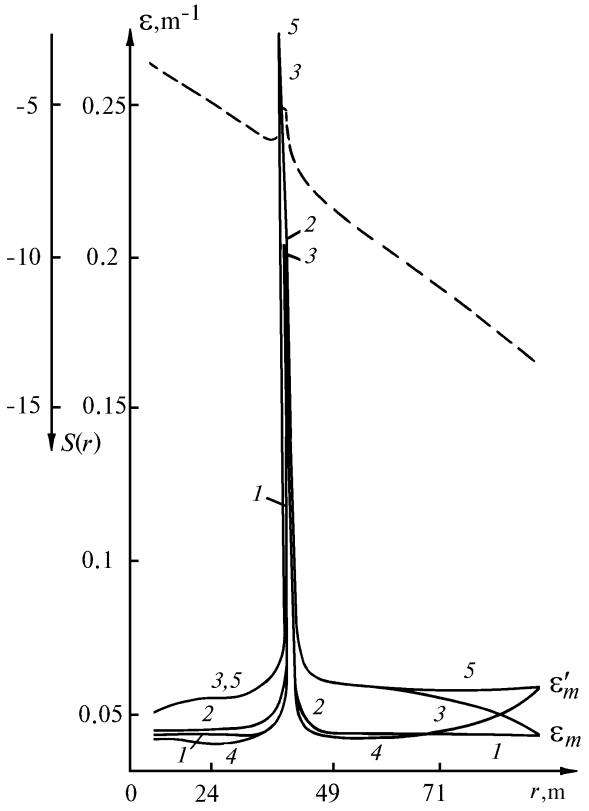

FIG. 5. The same as in Fig. 1 but for the Lorentz model profile $\varepsilon(r)$ (α = 5.0, δ = 7.5, r_0 = 40 m, *see Eq. (14)).*

As follows from the figures (curves *4* and *5*) the main errors of the profile reconstruction are due to the choice of the boundary conditions, in particular, $\varepsilon'_m = \hat{\varepsilon}(r_m)$. This is peculiar to the given inversion algorithm.

Our results allow us to draw the following conclusions:

First, compared with the known inversion algorithm, the obtained solution introduces essential corrections for the scattering effects. In this case, the accepted assumptions limiting the range of application of the proposed algorithm should be borne in mind.

Second, a peculiarity of the Klett algorithm (irrespective of scattering) is strong dependence of the profile on a choice of the value $\hat{\varepsilon}(r_m)$ (boundary conditions at the end point of sounding path). Obviously, this disadvantage can be overcome to a certain extent if we take into account a fact that variability of the extinction coefficient of oceanic medium decreased with depth and simultaneously the value of the extinction coefficient decreases monotonically. Extrapolation of the smoothed profile to the end point of the path will help one to approach the estimate $\hat{\varepsilon}(r_m)$ to its true value and thereby to decrease the error.

REFERENCES

1. A.F. Bunkin, D.V. Vlasov, and D.M. Mirkamilov, *Physical Foundations of Laser Aerosounding of the Earth's Surface* (Fan, Tashkent, 1987), 272 pp.
2. J.D. Klett, Appl. Opt. **20**, No. 2, 211–220 (1981).
3. J.D. Klett, Appl. Opt. **24**, No. 11, 1638–1643 (1985).
4. R.M. Measures, *Laser Remote Sensing* (John Willey and Sons, Inc., New York/Chichester/Brisbane/Toronto/Singapore, 1984).
5. B. Billard, R.H. Abbot, and M.F. Penny, Appl. Opt. **25**, No. 13, 2080–2088 (1986).
6. L.R. Bissonnette, Appl. Opt. **25**, No. 13, 2182–2185 (1986).
7. H.G. Hughes, J.A. Ferguson, and D.H. Stephens, Appl. Opt. **24**, No. 11, 1609–1613 (1985).
8. M. Käestner, Wiss. Mitt. Meteorol. Inst. Univ. Munchen, No. 56, 148–156 (1987).
9. J.A. Weinman, Appl. Opt. **27**, No. 19, 3994–4001 (1988).
10. L.S. Dolin and V.A. Savel'ev, in: *Sea Optics* (Nauka, Moscow, 1983), pp. 123–128.
11. O.D. Barteneva, Vestn. Akad. Nauk SSSR **1**, No. 12. 852 (1960).
12. A.S. Monin, ed., *Oceanic Optics*. I. *Physical Oceanic Optics* (Nauka, Moscow, 1983), 370 pp.
13. A.S. Monin, ed., *Oceanic Optics*. II. *Applied Oceanic Optics* (Nauka, Moscow, 1983), 235 pp.
14. D.V. Vlasov, V.N. Streltsov, and V.P. Slobodyanin, in: *Trudy IOFAN* (Nauka, Moscow, 1986), Vol. 1, pp. 39–59.